Synthesis, characterization, stability and structure of solid solutions between α-miargyrite(AgSbS$_2$) – smithite (AgAsS$_2$) and β- miargyrite - smithite

Morteza Razmara [1*]**, Richard Pattrick** [2]

[1] *Department of Geology, Ferdowsi University of Mashhad, Mashhad, Iran.*
[2] *Department of Earth Sciences, University of Manchester, Manchester, UK*
Corresponding author, e-mail: mortezarazmara@gmail.com

Abstract

Sulphosalts in the system AgSbS$_2$-AgAsS$_2$ have been experimentally investigated using dry methods. The solid solutions which form between α-miargyrite and smithite have different structures. The EPMA data for the solid solution series show that there is an inverse relation between Sb and As. The cell parameters of the solid solution between α-miargyrite and smithite increase up to about 50% of AgSbS$_2$ substitution in the smithite structure and then reveal a structural phase transition as a function of composition. Electron diffraction (TEM) data for α-miargyrite is consistent with the space group A2/a , but for the compositions Ag(As$_{0.1}$Sb$_{0.9}$)S$_2$ and Ag(As$_{0.3}$Sb0$_{.7}$)S$_2$, the phases do not show good Laue zones and Kikuchi lines and the symmetry could be either monoclinic or triclinic. The variation in the DW factor derived from the EXAFS spectra for the first shell of S atoms surrounding As in Ag(As$_{0.3}$Sb$_{0.7}$)S$_2$ tends to be smaller than for AgAsS$_2$ indicating that the As environment in Ag(As$_{0.3}$Sb$_{0.7}$)S$_2$ is more ordered than in Ag(As$_{0.5}$Sb$_{0.5}$)S$_2$ and AgAsS$_2$. This ordering indicates that with more substitution of Sb in AgAsS$_2$, the monoclinic (A2/a) Ag(As$_{0.5}$Sb$_{0.5}$)S$_2$ collapses around As atoms to a probable low-monoclinic or triclinic structure.

Key words: *Miargyrite, Smithite, Solid solution, Kikuchi lines, Laue zones, EXAFS*

Introduction

Phase relations in the Ag-As-S system have been studied by Jaeger & Van Klooster (1912) and they published a phase diagram for the join Ag$_2$S-As$_2$S$_3$. This phase diagram was later modified by Rolland (1970) (Fig. 1). A large number of investigations in chemistry, mineralogy, geochemistry and solid state physics have been carried out on the system Ag-S, Sb-S, Ag-Sb, Ag-Sb-S, Cu-Sb-S and Cu-Bi-S (Razmara *et. al.*, 1997).

AgAsS$_2$ exists as two polymorphs: The relatively rare minerals smithite (monoclinic, space group A2/a) and trechmannite (hexagonal, space group, R3). Synthetic trechmannite was made by Rolland (1968) by annealing smithite at 290 ºC for 315 hours and he showed that trechmannite is hexagonal with a possible space group R3. The equilibrium temperature of the smithite – trechmannite inversion has been determined to be 320 ± 5 ºC (Hall, 1966 , Rolland, 1970). Smithite melts congruently at 421 ± 2 ºC (Rolland, 1970). Smithite is the As-analogue of α AgSbS$_2$ and has the same A2/a space group [Hellner & Burzlaff, 1964]. Hall (1966) reported that a cubic form of AgAsS$_2$ (α-smithite) apparently isostructural with β-miargyrite, exists over a very restricted temperature stability range from 415 ºC to 421 ºC. The cubic form was not observed by Rolland (1970), Bryndzia & Kleppa (1989) or in this study.

Despite chemical differences there is a clear crystallographic relationship among the ternary compounds of the Ag-Sb-S and Ag-As-S systems. α-miargyrite and smithite have an identical A2/a space group. There is identical monoclinic symmetry between pyrostilpnite (low temperature form of Ag$_3$SbS$_3$) and xanthoconite (low temperature form of Ag$_3$AsS$_3$) as well as identical hexagonal symmetry between pyrargyrite (high temperature form of Ag$_3$SbS$_3$) and proustite (high temperature form of Ag$_3$AsS$_3$). It seems

that they tend to be mutually soluble in one another. Ghosal & Sack (1993) reported As-Sb exchange energies and non-idealities in smithite-miargyrite and proustite– pyrargyrite solid solutions.
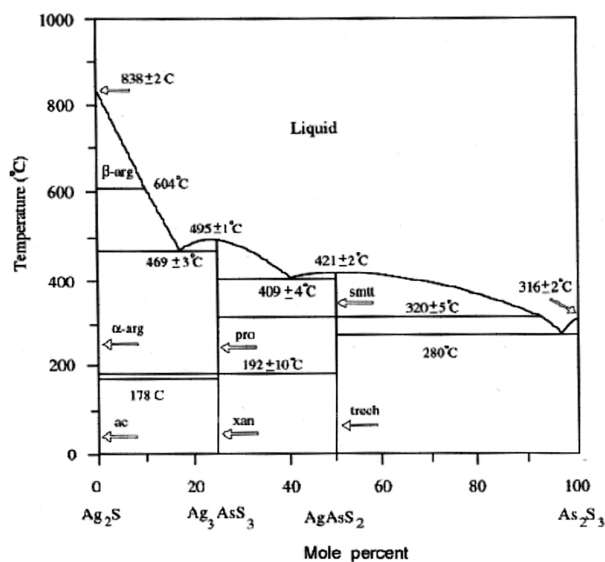

Figure 1: Phase relations along the join Ag_2S-As_2S_3 in the presence of vapour [modified from Rolland (1970); after Jaeger & Van Klooster, (1912)]. Abbreviations are as following : ac = acanthite; arg = argentite, xan = xanthoconite, pro = proustite, smt = smithite, trech = trechmannite. In this study smithite and trechmannite forms (in the center of diagram) are investigated.

In this study the syntheses of a solid solution series between α-miargyrite and β-miargyrite and the hypothetical cubic form of $AgAsS_2$ are reported as well as new phases in the low-temperatures solid solution series. The disordered structures in the solid solution are characterized by analogy with the structural relations of the end member phases, β-miargyrite and smithite.

Materials and methods
The compounds $Ag(As_xSb_{1-x})S_2$ in which x varied from 0 to 1 in increments of either 0.2 or 0.1 were synthesized using the conventional sealed evacuated silica glass capsules. Reagent Ag, Sb, As and S all with 99.99% purity, having the stoichiometric composition of the desired end products, were used in the preparation of the starting compositions. For the ordered and disordered solid solutions, samples with general

formula $Ag(As_xSb_{1-x})S_2$ (which x = 0.1 to 0.9) have been synthesized on both sides of T_c. Heat treatment was performed in furnaces in which the temperature was controlled to within ±3ºC. The charges were heated by two different procedures. In the first, the charges were heated at both 350ºC and 420ºC in a horizontal furnace for 8 days and quenched rapidly in liquid nitrogen. To expedite complete reaction tubes were opened and the contents were finely ground under acetone. They were then resealed in new tubes and reheated for 10 days at the same temperatures. In the second procedure the charges were heated above the melting temperature of the compounds, then either the temperature was decreased to below the α-β miargyrite phase transition and held at 340ºC for 5 days before being quenched in liquid nitrogen or the temperature was held at 420ºC for 3 days. The resulting products were examined by means of an optical microscope, XRD, EPMA, DSC, TEM and EXAFS in department of Earth sciences, The university of Manchester, UK.

XRD was used to check the nature of the reactions, the structure of the synthetic compounds and to obtain unit cell parameters. Experiments were made at room temperature on a computer controlled Philips PW 1730 diffractometere with a curved graphite crystal monochromator at 40 kV and 20 mA. Scans were made over the range 10-80º 2θ with 1º divergence and 0.1 mm scatter slits using Cukα radiation. The refinements were carried out using peak indexing in space group A2/a for miargyrite, smithite and the ordered solid solution series as well as Fm3m for β-miargyrite and the disordered solid solution series using the least square program. For EPMA and SEM studies, mineral standards for Sb, As, Ag and S were synthetic chalcostibite ($CuSbS_2$), arsenopyrite (FeAsS), matildite ($AgBiS_2$) and sphalerite (ZnS) respectively. The sample compositions were determined by WDS method using a Cameca Camebax electron probe, controlled by a link systems AN 10000 computer and analyzing system. The following

run conditions were employed: take off angle (40º), a beam diameter of 2-3 μm, carbon coating thickness (20 nm), accelerating voltage 20 kV.

Ultra thin sections of miargyrite were prepared from doubly polished petrographic thin sections (~μm). 3 mm discs were cored out and thinned by ion bombardment with 5 kV Ar-ions impinging at a 15º angle to the sample. One of the specimens was carbon-coated on both sides to improve electrical conductivity. Another sample was embedded in indium. The TEM investigations were performed with a Philips CM200 electron microscope operating at 200kV. Heating experiments were performed using a heating stage to heat the sample close to the phase transition temperature α-miargyrite to β-miargyrite.

Results

Results obtained from SEM and EPMA analyses showed that the phases produced for solid-solution series were homogeneous and stoichiometric with a formula $Ag(As_xSb_{1-x})S_2$ in which X varies from zero to 1 (Table 1). The only exception was between $Ag(As_{0.8}Sb_{0.2})S_2$ and $AgAsS_2$ where a miscibility gap in the solid solution between β-miargyrite and smithite occurs above 370 ºC.

For synthetic α-miargyrite (A2/a space group) and β-miargyrite (Fm3m), the diffraction patterns obtained at room temperature were compared with those in the literature. All of the peaks were indexed, confirming that no impurity phases were present. The X-ray powder pattern of synthetic smithite matched on that of Sugaki *et al.* (1978), except for the less intense peaks, although the cell parameters are close. The X-ray powder diffraction patterns for members of the solid-solution series had sharp peaks, suggesting that the products are chemically homogeneous and single phases.

The diffraction patterns of the nominal compositions for low-temperature forms $Ag(As_{0.9}Sb_{0.1})S_2$, $Ag(As_{0.7}Sb_{0.3})S_2$ and $Ag(As_{0.5}Sb_{0.5})S_2$ can be indexed based on the smithite unit cell and thus the smithite (monoclinic) structure can be considered the aristotype for the series, with the other members being derived from it by the ordered substitution of Sb for As in solid solution between smithite and miargyrite. For compositions with Sb>0.5 mole fraction, the X-ray patterns can not be indexed based on the α-miargyrite or smithite unit cells (unknown structures).The solid solution series having a monoclinic structure [$AgAsS_2$ to $Ag(As_{0.5}Sb_{0.5})S_2$] can be distinguished from unknown structures by its different physical properties (e.g. optical properties).

Table 1: EPMA analysis of synthetic end-members, $AgAsS_2$, $AgSbS_2$ and $Ag(As_xSb_{1-x})S_2$.

Phase	Weight percent				Total	Theoretical Formula	Experimental Formula
	Ag	As	Sb	S			
Smithite*	43.58	31.53	-	26.21	101.32	$AgAsS_2$	$Ag_{1.00}As_{1.03}S_2$
α -S.S.**	45.48	26.97	5.22	25.01	102.69	$Ag(As_{0.9}Sb_{0.1})S_2$	$Ag_{1.08}(As_{0.92}Sb_{0.11})S_2$
α -S.S.**	42.01	20.23	14.90	24.43	101.56	$Ag(As_{0.7}Sb_{0.3})S_2$	$Ag_{1.02}(As_{0.71}Sb_{0.32})S_2$
α -S.S.**	39.59	15.29	21.68	23.55	100.12	$Ag(As_{0.5}Sb_{0.5})S_2$	$Ag_{1.00}(As_{0.56}Sb_{0.49})S_2$
α -S.S.**	39.68	8.90	31.35	22.63	102.63	$Ag(As_{0.3}Sb_{0.9})S_2$	$Ag_{1.04}(As_{0.34}Sb_{0.23})S_2$
α -S.S.**	38.17	2.54	38.54	21.62	100.88	$Ag(As_{0.1}Sb_{0.9})S_2$	$Ag_{1.05}(As_{0.10}Sb_{0.94})S_2$
α-miargyrite*	37.37	-	41.03	20.88	99.28	$AgSbS_2$	$Ag_{1.06}Sb_{1.04}S_2$

The cell parameters and cell volumes show smooth increases with increasing Sb content in $AgAsS_2$ (up to 60% Sb content), but show a very sharp decrease as a result of the structural phase transition (Figs. 2 and 3). However, note that the expansion is highly anisotropic with that

along b being only 18% of those in the a and c directions, up to the $Ag(As_{0.4}Sb_{0.6})S_2$ composition, after which b shows a dramatic change (Fig. 2 and Table 2).

The cell parameters and cell volumes of the solid solution between β-miargyrite and smithite show a linear decrease with increasing As. This measured trend for the cell parameters is expected, as Sb [effective ionic radius (IR) of 0.76 Å (Shannon, 1976)] is larger than As [IR of 0.58 Å (Shannon, 1976)].

In the DSC experiments on pure end member α-miargyrite, the first strong endothermic reaction was initiated at about 381 ℃ (Fig. 4) and has an energy of 12.5 kJ/mol. Previous work (Sugaki *et al.* 1978) suggests that this peak represents the phase transition from the monoclinic to the cubic structure. In smithite $(AgAsS_2)$, the strong endothermic reaction initiated at 415℃ represents the congruent melting of smithite. Above the melting point, the TG curve showed a sharp decrease in weight due to the decomposition of $AgAsS_2$. A very weak endothermic reaction starting at 413

℃ might be related to an inversion point from monoclinic to hypothetical cubic $AgAsS_2$. Note that Hall (1966) reported a cubic form $AgAsS_2$ (from 415 ℃ to 421 ℃).The hypothetical cubic form was not detected by XRD experiments.

The presence of 10% $AgAsS_2$ in end member $AgSbS_2$ increases the transformation temperature to 397 ℃, with the transformation energy decreasing to 11.8 kJ/mole (compared to miargyrite) and the melting point to 496 ℃. With 30% of As component, the transformation energy (10.9 kJ/mole) and melting point (454℃) decrease further but the transformation temperature remains at 397℃. With more than 50% of As component, no transformation was detected by DSC at the heating rate used (10 ℃/min). Apparently the kinetics of the nucleation and growth are too sluggish for the reaction to proceed on the time scale of the DSC experiments. However, it was not possible to synthesise the cubic phase for the compositions between $Ag(As_{0.9}Sb_{0.1})S$ ₁and $AgAsS_2$ in high temperature.

Table 2: Some crystallographic data for synthetic silver, antimony and arsenic sulphide $Ag(As_xSb_{1-x})S_2$ at high temperatures.

Exp. No.	Compound	Space group	a (Å)	b (Å)	c (Å)	β (Å)	V (Å)
1E	$β$-$AgSbS_2$	Fm3m	5.6565	-	-	-	180.9853
10As	$Ag(As_{0.1}Sb_{0.9})S_2$	Fm3m	5.6456(6)	-	-	-	179.9411
30As	$Ag(As_{0.3}Sb_{0.9})S_2$	Fm3m	5.6152(4)	-	-	-	177.0499
50As	$Ag(As_{0.5}Sb_{0.5})S_2$	Fm3m	5.6023(5)	-	-	-	175.8325
70As	$Ag(As_{0.7}Sb_{0.3})S_2$	Fm3m	5.5685(8)	-	-	-	172.6691
90As	$Ag(As_{0.9}Sb_{0.1})S_2$	Fm3m	5.5470	-	-	-	170.677
100As	$AgAsS_2$	Fm3m	5.5346	-	-	-	169.535
33C	$AgAsS_2$	A2/a	17.224	7.786	15.187	101.11	1998.4997
10Sb	$Ag(As_{0.9}Sb_{0.1})S_2$	A2/a	17.286(4)	7.793(3)	15.273(1)	101.08(3)	2019.072
30Sb	$Ag(As_{0.7}Sb_{0.3})S_2$	A2/a	17.368(5)	7.830(3)	15.359(1)	101.16(4)	2049.196
50Sb	$Ag(As_{0.5}Sb_{0.5})S_2$	A2/a	17.42(2)	7.823(5)	15.387(2)	100.87(1)	2060.604
70Sb	$Ag(As_{0.3}Sb_{0.9})S_2$	?	?	?	?	?	?
90Sb	$Ag(As_{0.1}Sb_{0.9})S_2$	?	?	?	?	?	?
100Sb	$α$-$AgSbS_2$	A2/a	13.162	4.411	12.820	98.38	

The TEM investigations of α-miargyrite showed that it was homogeneous at the scale of 10 nm. The electron diffraction confirmed that the α-miargyrite structure is consistent with space group, A2/a with a=13.2, b=4.4, c=12.9 Å and β=98.5.
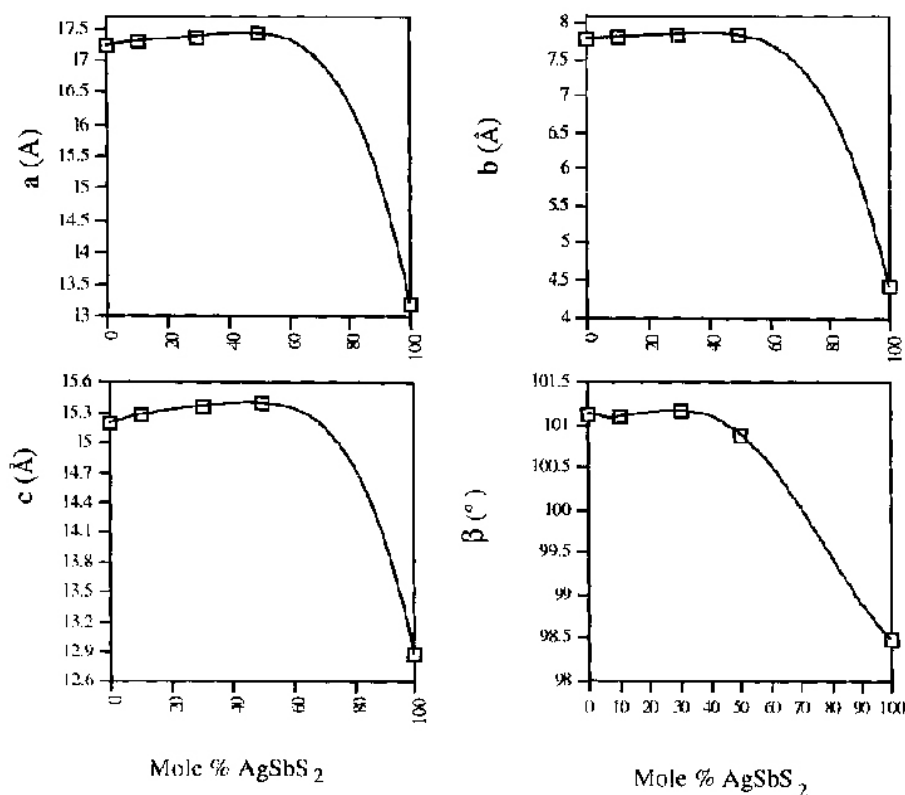
Figure 2: Cell parameter variations (a, b, c and β) with composition in the solid solution series between α-AgSbS$_2$ and smithite. Note that the lack of data for the phases between Ag(As$_{0.5}$Sb$_{0.5}$)S$_2$ and Ag(As$_{0.1}$Sb$_{0.9}$)S$_2$ is due to unknown structure for these phases.


Mole % AgSbS$_2$
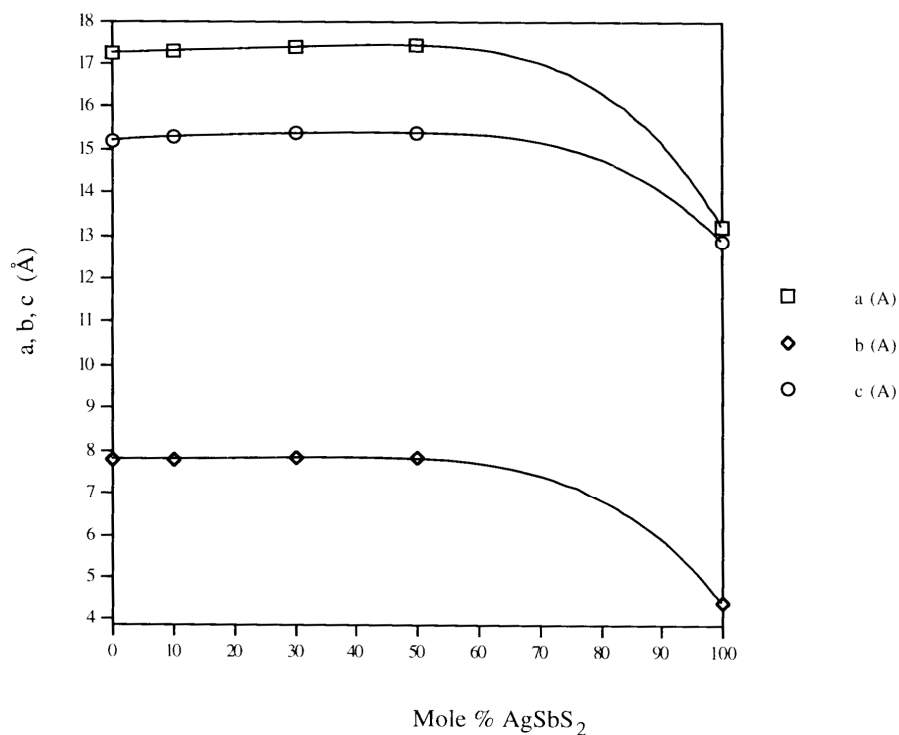
Figure 3: Variations in Cell parameters of synthetic solid solution between α-miargyrite and smithite.
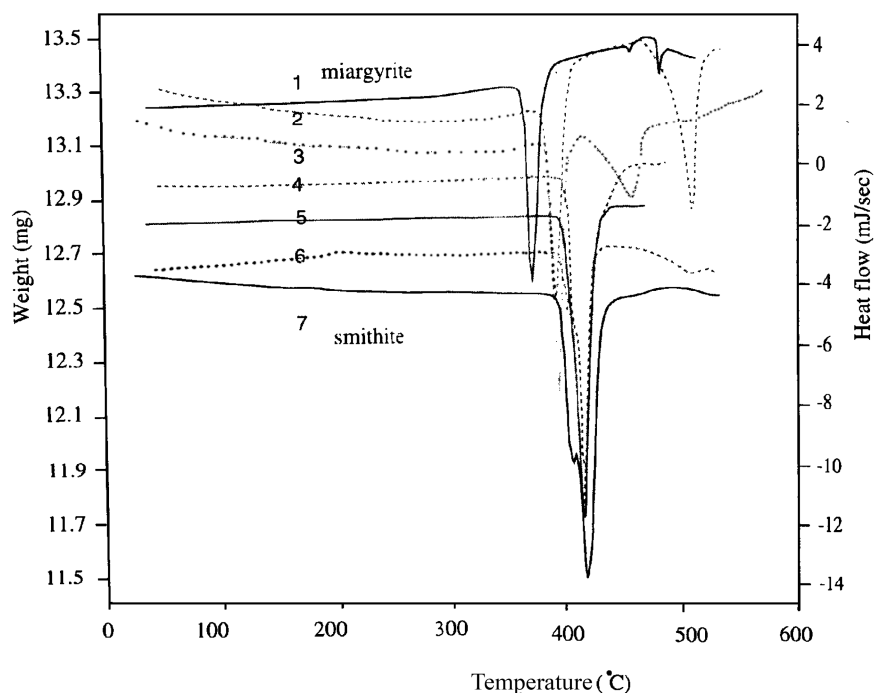
Figure 4: DSC data for miargyrite, smithite and members of the solid solution series between β-AgSbS$_2$ and smithite. The strong endothermic reaction (No. 7) initiated at 415°C represents the congruent melting of smithite (AgAsS$_2$). A final endothermic reaction (No. 1) is related to the congruent melting reaction of AgSbS$_2$.

The dark field images of Ag(As$_{0.1}$Sb$_{0.9}$)S$_2$ showed faint striations in the crystals that are likely to be related to a modulated structure. In the electron diffraction patterns (Fig. 5), sets of bright spots form a centered square. This would correspond to a pseudo-cubic cell with a=5.5 Å. This is evidence of the effect of As in the structure of α-miargyrite. The symmetry looks to be monoclinic or triclinic. All the phases are poorly crystalline and do not show good Laue zones and Kikuchi lines. This makes it difficult to explore reciprocal space to find low-index sections.

The As EXAFS data for the end-members, Ag(As$_{0.5}$ Sb$_{0.5}$)S$_2$ and Ag(As$_{0.3}$Sb$_{0.7}$)S$_2$ are shown in Table 3. Refined As K-edge and Ag K-edge EXAFS spectra for the end member smithite are shown in Figs. 6a and 6b. The EXAFS spectra and Fourier transform of Ag(As$_{0.5}$ Sb$_{0.5}$)S$_2$ and AgAsS$_2$ are similar (Fig. 7) and reveal the As to be in 3-fold co-ordination in both samples, but different EXAFS spectra and Fourier transform are observed between Ag(As$_{0.5}$ Sb$_{0.5}$)S$_2$ and Ag(As$_{0.3}$Sb$_{0.7}$)S$_2$ (Fig. 8) This is clear evidence of a phase transition as a

function of the composition in the AgAsS$_2$ structure with more than 60% Sb content.

The mean As-S bond lengths in Ag(As$_{0.5}$ Sb$_{0.5}$)S$_2$ and Ag(As$_{0.3}$Sb$_{0.7}$)S$_2$ are equal to 2.28 Å and 2.27 Å, respectively, revealing no significant structural variations to those in end member (AgAsS$_2$).
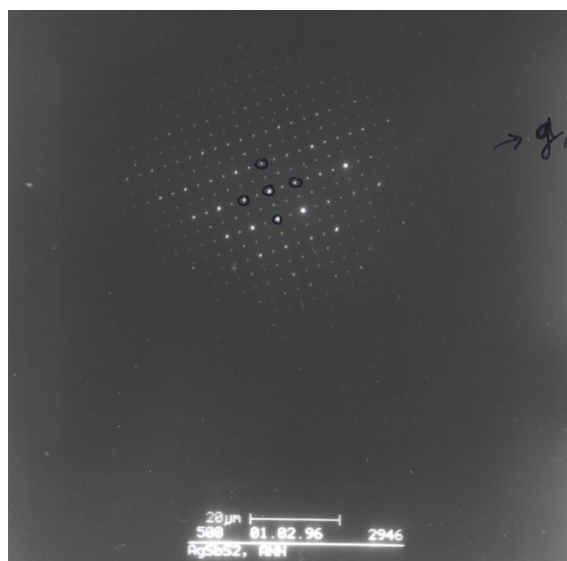

Figure 5: Electron diffraction patterns of Ag(As$_{0.1}$Sb$_{0.9}$)S$_2$. Sets of bright field spots ringed from a centered square. This would correspond to a pseudo-

cubic cell with a = 5.5 Å.

Table 3: Refined EXAFS data of end-members, $Ag(As_{0.5}Sb_{0.5})S_2$ and $Ag(As_{0.3}Sb_{0.7})S_2$.

Exp. No.	Compositions	EXAFS results					
		R (Å)[a]	N[b]	$2\sigma^2$ (Å)[c]	R (Å)[d]	N[e]	$2\sigma^2$ (Å)[f]
1	$AgAsS_2$	R1 = 2.29 R2= 3.46 R3= 3.53 R4= 3.58 R5= 3.92	N1 = 2.0 N2= 2.0 N3= 2.0 N4= 2.0 N5= 4.0	0.006 0.015 0.015 0.019 0.047	2.463	2	0.017
2	$Ag(As_{0.5}Sb_{0.5})S_2$	2.28	3	0.007	-	-	-
3	$Ag(As_{0.3}Sb_{0.7})S_2$	2.27	3	0.001	-	-	-
4	α-$AgSbS_2$	-	-	-	2.47	3	0.056
5	β-$AgSbS_2$	-	-	-	2.55	3?	0.041

a : Average bond lengths for co-ordination shells: R1 = As-S; R2 = As-S; R3 = As-As;   R4 = As-Ag and R5= As-Ag.

b : Fixed co-ordination number for As-S bond.

c : Debye Waller factor for As-S bond ($\pm$ 0.002 Å).

d : Average Ag-S bond lengths for the first co-ordination shell ($\pm$ 0.01 Å).

e : Fixed co-ordination number for Ag-S bond.

f : Debye Waller factor for Ag-S bond ($\pm$ 0.002 Å).

Discussion

Four main factors on an atomic scale affect the ranges of isostructural solid solutions. They are size difference, charge, covalency and electronic factors (Navrotsky, 1985). The size difference between Sb and As is the most important factor; it causes a strain in the solid solution as the difference in the ionic size of Sb and As is greater than 15%. The larger the difference between the size of Sb and the As site in which it is substituted, the more incompatible is the ion in that site. In the solid solution between α-miargyrite and smithite, the compositions between $Ag(As_{0.5}Sb_{0.5})S_2$ and $AgSbS_2$ have a different structure from other members of the solid-solution. However, all of the solid solution series compositions between β-miargyrite and smithite are consistent with space group Fm3m. The extent of the solid solution in the different polymorphs (cubic and monoclinic) of $AgSbS_2$ shows that crystallographic symmetry is another factor which controls the amount of substitution of As in $AgSbS_2$. An attempt has been made to determine the phase boundaries between smithite and β-miargyrite by assuming an ideal solid-solution between them. The transformation from α-miargyrite-smithite solid-solution to β-miargyrite-smithite was found to be completely reversible between the composition of $Ag(As_{0.9}Sb_{0.1})S_2$ and $AgSbS_2$. There is a possible eutectic at 392 ℃ at a composition $Ag(As_{0.8}Sb_{0.2})S_2$.

The solid solution between ordered α-miargyrite and smithite extends from $AgAsS_2$ to $Ag(As_{0.4}Sb_{0.6})S_2$, without strain causing a structural phase transition as a function of composition. The cell expansion reaches a limit at $Ag(As_{0.4}Sb_{0.6})S_2$ with a structural change at this composition to a monoclinic or triclinic structure. The reason for this limit might be the strain on the structure after half the Sb atoms (ionic radius of 0.76 Å) are replaced by the significantly smaller As atoms (ionic radius of 0.58 Å). The lower radius of As might cause a higher mobility relative to Sb, and the ordering of Sb on the As sites of $AgAsS_2$ may be the rate-determining step in the overall cation-ordering process in these structures. When more than 50% of As atoms are replaced by Sb atoms in the smithite structure, the sum of the strain fields becomes so strong that a structural phase transition occurs as a function of composition. However, in the α-miargyrite structure, substitution of a few percent of As in Sb sites causes such strain that the structure collapses to the lower space group. At higher

temperatures, the low-symmetry solid-solution series transforms to a galena structure with a density increase of around 3%. It was expected that the smaller ion, As, could be substituted in the bigger Sb sites of α-miargyrite more easily than substitution of the bigger Sb in the smaller As site. Arsenic substitutes very easily in the Sb sites of the higher temperature form (β-miargyrite) without changing the structure but

at lower temperatures, substitution of As in Sb sites is accompanied by structural changes. This showed that the substitution of As and Sb in the crystal structure of chalcogenides not only is controlled by the physical and chemical character of the elements, but also by more important thermodynamical factors such as temperature.
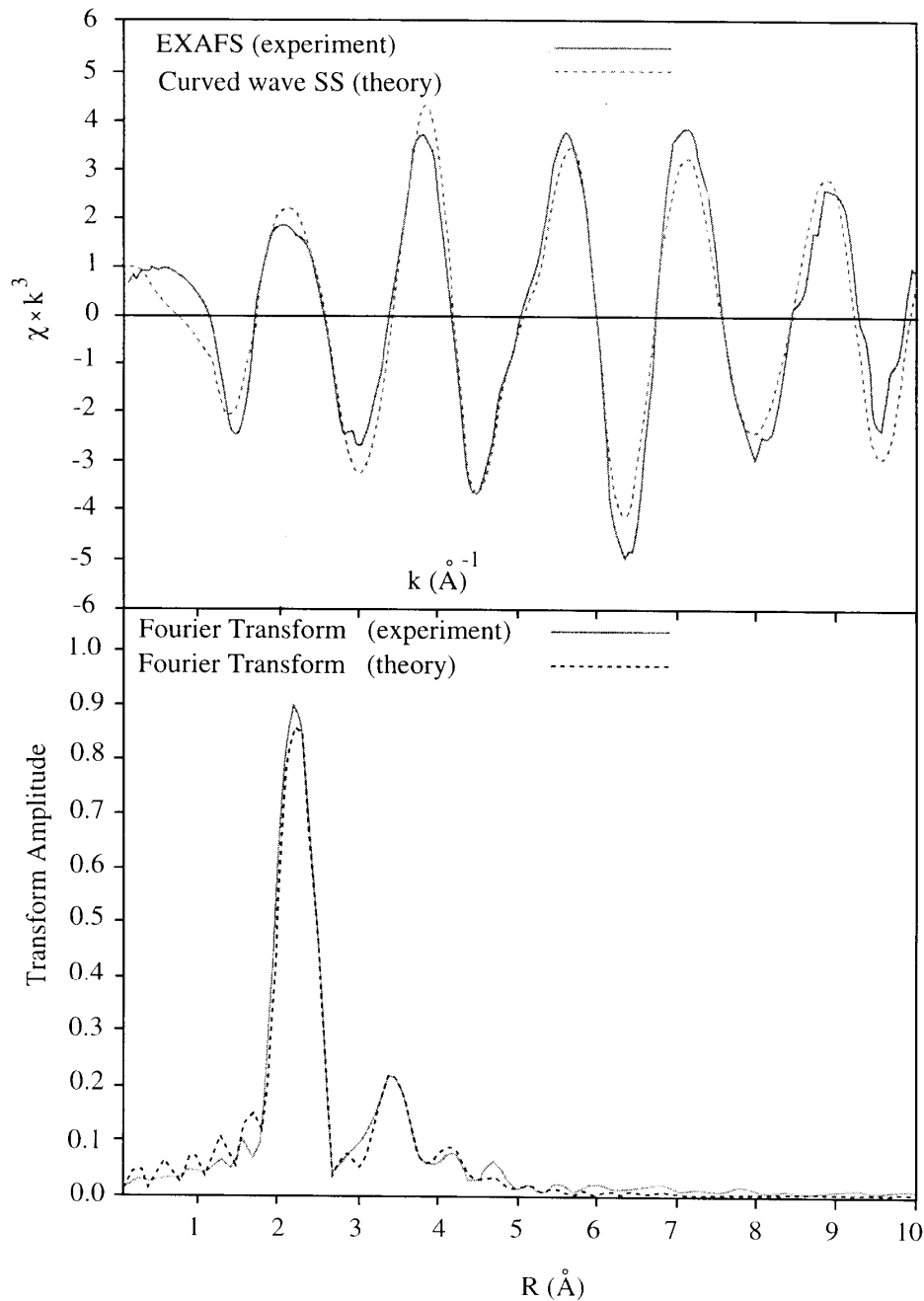
Figure 6a: As K-edge EXAFS (top) and Fourier transform (bottom) for $Ag(As_{0.3}Sb_{0.9})S_2$ (top) and $AgAsS_2$.
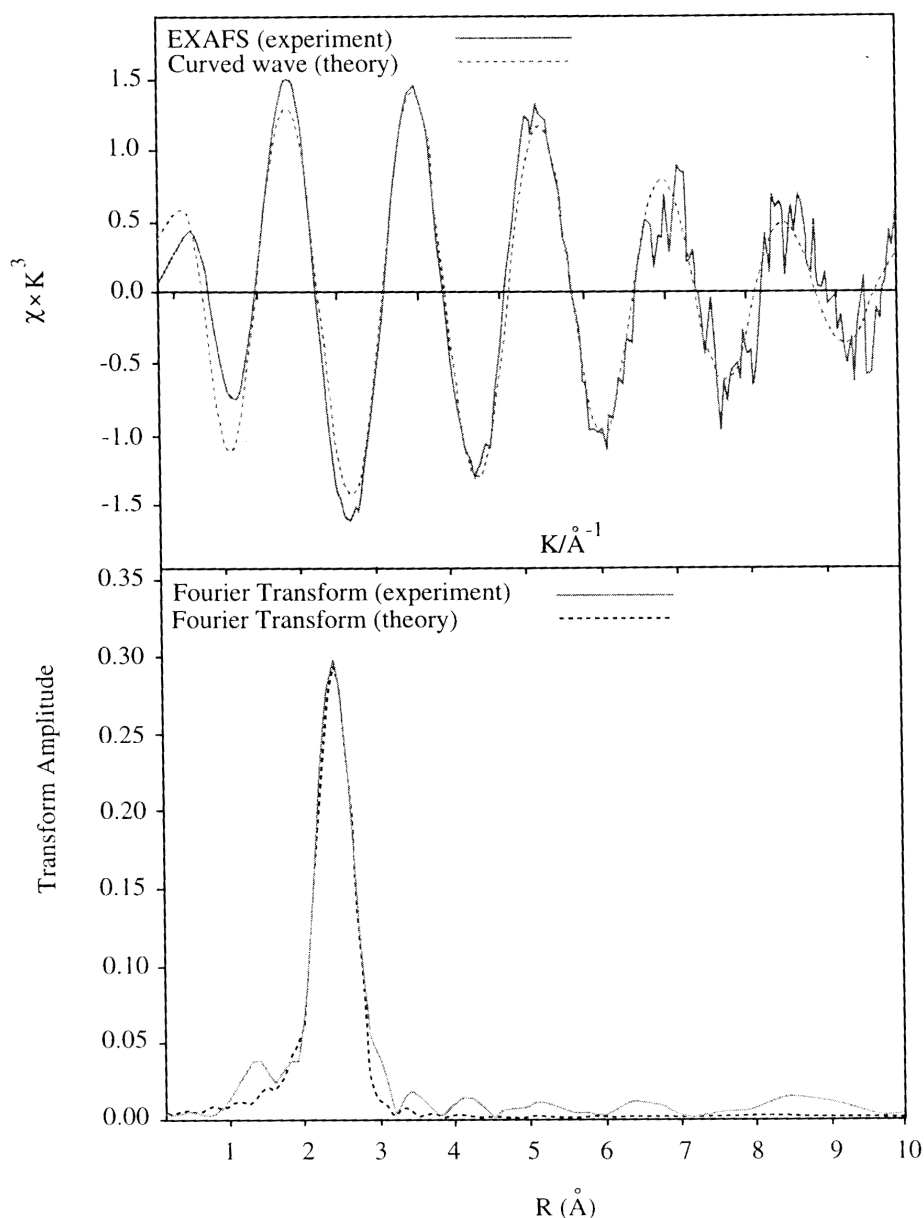
Figure 6b: Ag K-edge EXAFS (top) and Fourier transform (bottom) for end member $AgAsS_2$.

The cell parameters of the solid solution between β-miargyrite and smithite increase linearly with increasing Sb. The results demonstrate that solid solution exists between the two end members, α-miargyrite and smithite, and an extensive solid solution based on the β-miargyrite exists at higher temperatures. In the solid solution between α-$AgSbS_2$ and smithite, the percentage change in b is five times less than that for a and c [between $AgAsS_2$ and $Ag(As_{0.5}Sb_{0.5})S_2$].
In the synthesized conditions, the results indicated that the cubic Fm3m structure of $AgAsS_2$ and $Ag(As_{0.9}Sb_{0.1})S_2$ is thermodynamically unstable. However, if the thermodynamic conditions (pressure, temperature and fugacity) for the formation of the phases are changed, these phases may be formed stably. The cell parameters and cell volumes of hypothetical cubic forms of $AgAsS_2$ and $Ag(As_{0.9}Sb_{0.1})S_2$ have been predicted by analogy with the a-cell parameter of the other cubic forms of the solid solution series (between β-miargyrite and smithite).
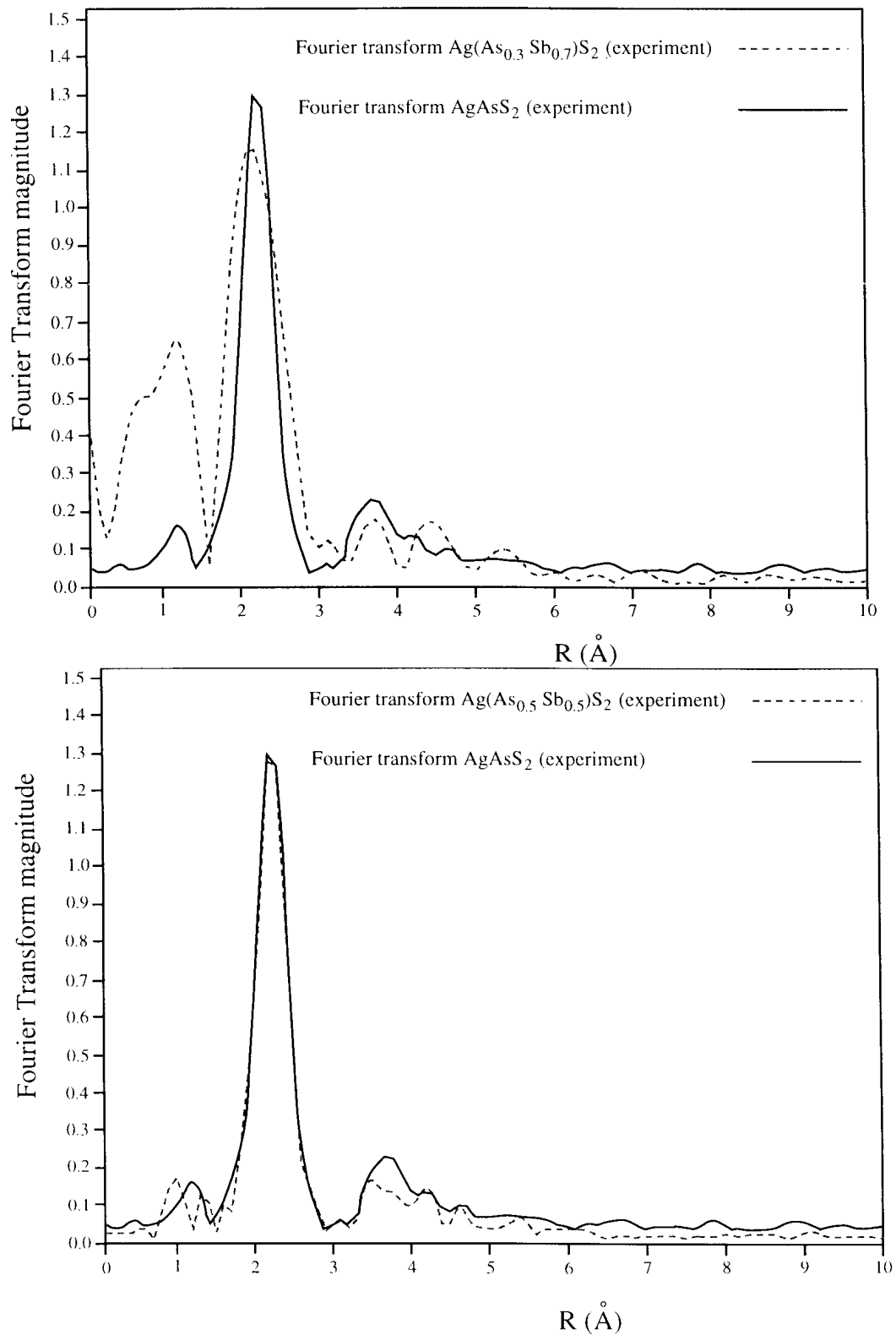
Figure 7: The comparison between the experimental Fourier transform for $AgAsS_2$-$Ag(As_{0.3}Sb_{0.7})S_2$ (top) and $AgAsS_2$-$Ag(As_{0.5}Sb_{0.5})S_2$ (bottom).
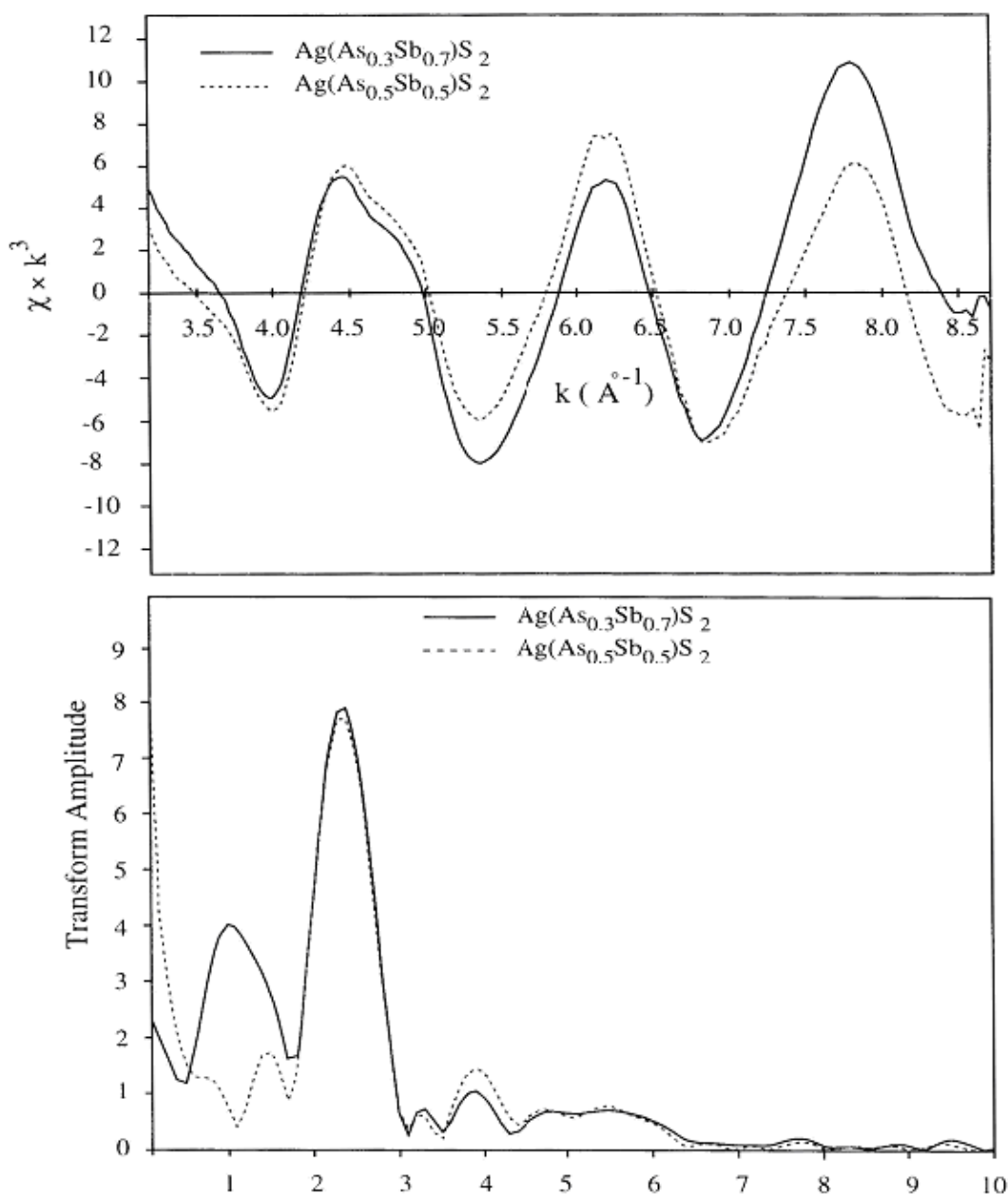
Figure 8: EXAFS spectra for $Ag(As_{0.3}Sb_{0.7})S_2$ and $Ag(As_{0.5}Sb_{0.5})S_2$ (top), Fourier transform spectra for $Ag(As_{0.3}Sb_{0.9})S_2$ and $Ag(As_{0.5}Sb_{0.5})S_2$ (bottom).

The variation in the Debye-Waller factor derived from the EXAFS spectra for the first shell of S atoms surrounding As in $Ag(As_{0.3}Sb_{0.7})S_2$ tends to be smaller than for $AgAsS_2$ and $Ag(As_{0.5}Sb_{0.5})S_2$ (Table 3) indicating that the As environment in $Ag(As_{0.3}Sb_{0.7})S_2$ is more ordered than in $Ag(As_{0.5}Sb_{0.5})S_2$ and $AgAsS_2$. This ordering indicates that with more substitution of Sb (>60%) in $AgAsS_2$, the monoclinic (A2/a) $Ag(As_{0.5}Sb_{0.5})S_2$ collapses around As atoms to a probable low-monoclinic or triclinic structure. In $Ag(As_{0.5}Sb_{0.5})S_2$ there is some kind of As and S ordering, but in $Ag(As_{0.3}Sb_{0.7})S_2$ As, S ordering can proceed until the fully ordered structure is formed. As, S ordering is promoted by the displacive distortion of the monoclinic structure and occurs following higher Sb substitution in $Ag(As_{0.4}Sb_{0.6})S_2$.

Conclusions

Complete solid solution series exists between β-

miargyrite and smithite as well as an extensive solid solution between smithite and α-miargyrite with a gap between smithite and 10% α-miargyrite.

The form of the experimental liquidus and solidus are indicated non-idealities in the $AgSbS_2$ – $AgAsS_2$ solid solution series.

Unknown complex structures [$Ag(As_{0.1}Sb0_{.9})S_2$ and $Ag(As_{0.3}Sb_{0.7})S_2$] appeared in the solid solution between smithite and α-miargyrite may be related to ordering of As and Sb with the addition of Sb to smithite.

Inverse relationships between As and Sb in the solid solution between smithite and miargyrite demonstrate that As and Sb can be exchanged in the compounds with similar structural compositional relationship. As a result, it is predicted that there is a solid solution between two isomorphs pyrargyrite (Ag_3SbS_3) with space group R3c (161) and proustite (Ag_3AsS_3) with the same space group of pyrargyrite.

References

Bryndzia, L.T., Kleppa, O.J., 1989. Standard molar enthalpies of formation of sulfosalts in the Ag-As-S system and thermochemistry of the sulfosalts of Ag with As, Sb and Bi. Am. Mineral. 74, 243-249.

Ghosal, S., Sack, R.O., 1993. As-Sb exchange energies and non-idealities in smithite-miargyrite and proustite-pyrargyrite solid solutions. Geological Society Am., 1993 annual meeting. Abstracts with programs, 25, 96.

Hall, H.T., 1996. The systems Ag-Sb-S, Ag-As-S and Ag-Bi-S: phase relations and mineralogical significance. Unpublished Ph.D. thesis, Brown University, 172 pp.

Hellner, E., Burzlaff, H., 1964. Die struktur des smithits $AgAsS_2$. Naturwissenschaften, 51, 35-36.

Jaeger, F.M., Van Klooster, H.S., 1912. Studien uber naturliche und kunstliche sulfantimonite und sulfoarsenite. Zeit. Anorg. Chemie. 78, 245-269.

Navrotsky, A., 1985. Crystal chemical constraints on the thermochemistry of minerals. In "Microscopic to Macroscopic, Atomic Environments to Mineral Thermodynamics. Reviews in Mineralogy, 14, 225-275.

Razmara, M. F., Henderson, C. M. B., Pattrick, R. A. D., Bell, A. M. T., Charnock, J. M., 1997. The crystal chemistry of the solid solution between chalcostibite ($CuSbS_2$) and emplectite ($CuBiS_2$). Mineralogical Magazine, 61, 79-88.

Rolland, G.W., 1968. Synthetic trechmannite. Am. Mineral., 53, 1208-1214.

Rolland, G.W., 1970. Phase relations below 575° C in the system Ag-As-S. Econ. Geol., 65, 241-252.

Shannon, R.D., 1976. Revised effective ionic radii and systematic studies of interatomic distances in halides and chalcogenedies. Acta Cryst., A32, 571-767.

Sugaki, A., Shima, H., Kitakaze, A., 1978. the phase equilibrium of the system copper-bismuth- sulfur below 400° C, especially the relation between emplectite and cuprobismutite. Sulfosoli, platinovye miner., Rudn. Mikrosk. Master., Sezda MMA, 11th. (pub. 1980).